Studies on Radioemission from EAS by the GUCR group

Datta (Mrs) Pranayee [1], Baishya (Mrs) Runima [2] & Roy Sinha (Mrs) Kalpana [3]

[1] Reader, Deptt of Physics & i/c, Deptt. of Electronics Science; Gauhati University, Guwahati- 781014,Assam ,India.
[2] Lecturer, Deptt of Physics, Pragjyotish College , Guwahati, Assam ,India
[3] Lecturer, Deptt of Physics, Assam Engineering Institute, Guwahati, Assam ,India

Different characteristics of LF-MF-HF-VHF Radioemission(RE) from EAS have been studied theoretically as well as experimentally by the Gauhati University Cosmic Ray (GUCR) group since 1970.

Experimental works of GUCR group : EAS array and experimental arrangement for RE investigation used by GUCR group is given in fig 1 & 2. The general features of the EAS observed by this array viz lateral distribution of the electron component,age parameter distribution,shower size distribution and zenith angle distribution are found to be consistent with the well known characteristics of EAS .Fieldstrengths of RE obtained at different frequencies are given in table 1. Correlation between simultaneously produced radiopulses were studied for different frequency pairs during the period 1979-1992. Results of this series of experiment are given in table 2.

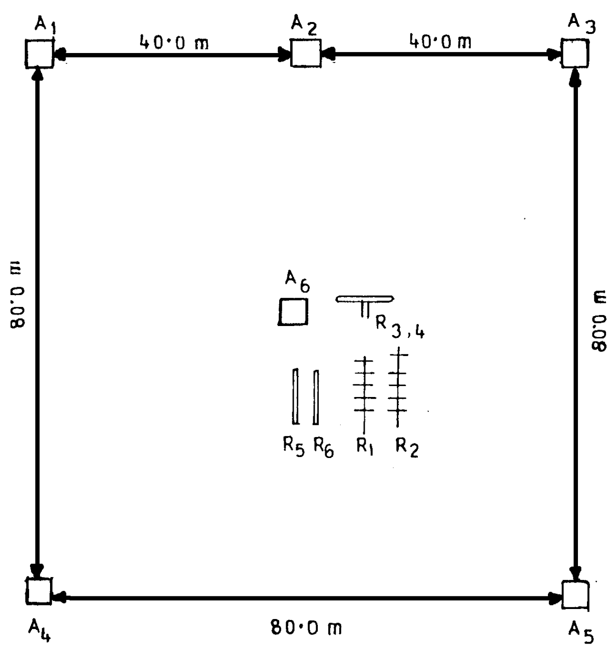

Fig. 1 - Array diagram of detectors.
A_{1-6} = Particle detectors.
R_{1-6} = Radio pulse detectors.

TABLE : 1. Fieldstrength of radio pulses at different frequencies

Frequency in MHz	Normalised fieldstrength in $\mu Vm^{-1} MHz^{-1}$ (experimental)	
	Datta (1987)	Barthakur (1978)
2	493.6 $\pm$ 188.5	-
9	138.07 $\pm$ 38.9	-
44	-	3.70 $\pm$ 0.2
60	-	3.40 $\pm$ 0.2
80	-	2.20
110	1.96 $\pm$ 0.28	-
220	0.403 $\pm$ 0.124	-

TABLE : 2. Correlation coefficient 'x' for different frequency pairs.

Experiment	Frequency pair in MHz	Correlation Coefficient 'x'	t-test of significance at 1% & 5% levels.	Remarks regarding production mechanism (PM)
Barthakur (1979)	(60-80)	+ 0.68	Significant at both the levels of test	PM at 60 MHz is similar to that at 80 MHz.
Sarma (1981)	(60-110)	- 0.35	- do -	PM at 60 MHz is different from that at 110 MHz.
Sarma (1981)	(60-220)	- 0.31	- do -	PM at 60 MHz is different form that at 220 MHz
Borah (1983)	(60-9)	+0.38	- do -	PM at 60 MHz is similar to that at 9 MHz.
Datta (1987)	(2-110)	- 0.69	- do -	PM at 2 MHz is different from that at 110 MHz.
Datta (1987)	(9-220)	- 0.28	- do -	PM at 9 MHz is different from that at 220 MHz
Kalita (1992)	(2-220)	- 0.45	- do -	PM at 2 MHz is different from that at 220 MHz.
Kalita (1992)	(9-110)	- 0.41	- do -	PM at 9 MHz is different from that at 110 MHz.

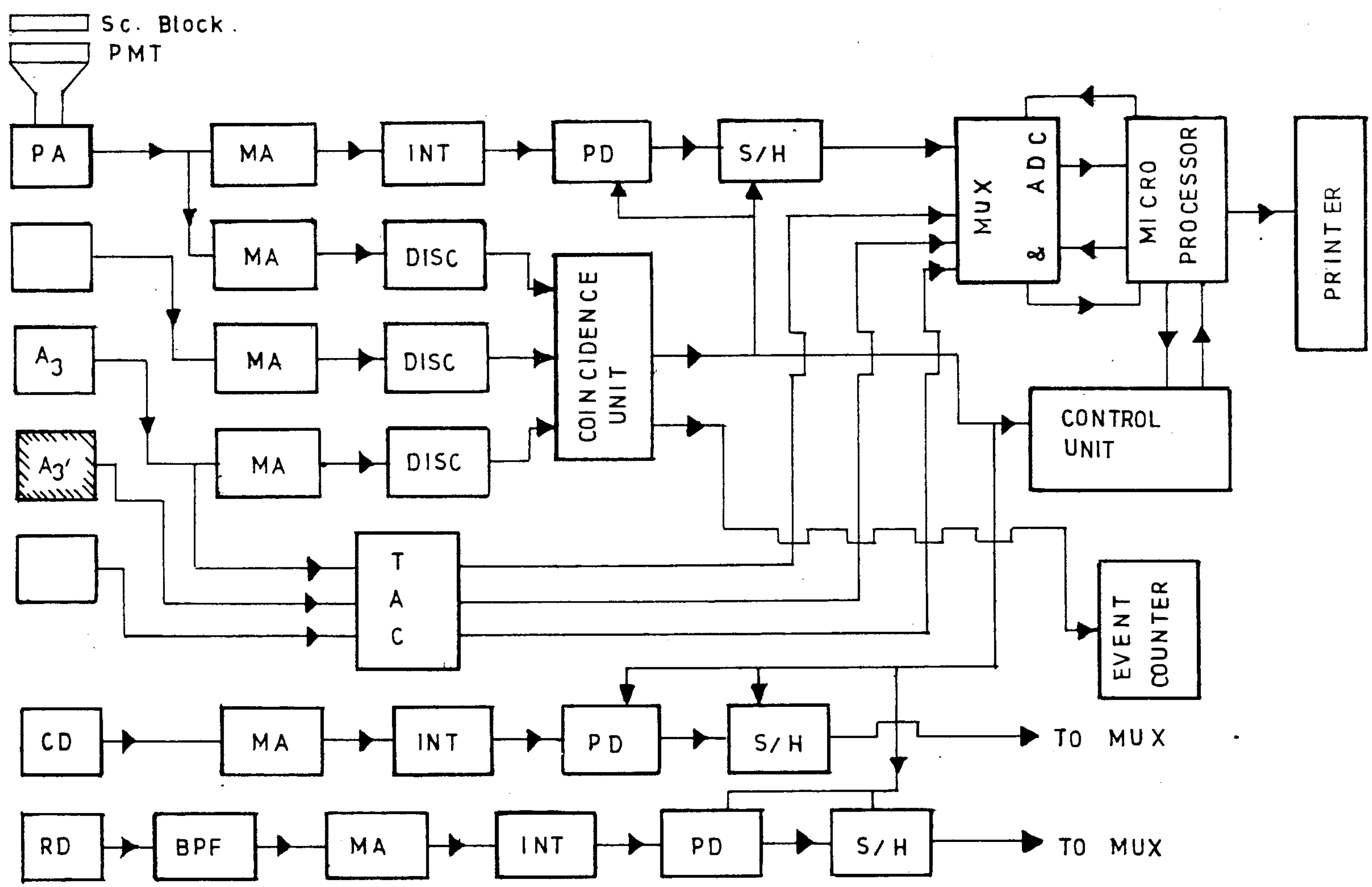

Fig. 2 - Flow diagram of the experimental set-up

Theoretical works of GUCR group: Using Castagnoli et al's (1) modifications of Kahn & Larche's (2) model, fieldstrengths were calculated for primary energy $E_p = \sim 10^{16}$ eV at a point inside the shower disc. The procedure is detailed below.

For a point lying inside the disc of charges of radius R_0 at a distance R from the axis, the point will be an outer one with respect to the disc of radius R and an inner one with respect to the annular ring of inner radius R and outer radius R_0. Accordingly, effects of the disc of radius R and the annular ring were taken into account.

Current field at a distance R from the $_{\text{Axis}}$ ($R<R_0$)

a) Current field due to the disc radius R is given by

$$E_c^{/}(R) = -\frac{ke10^5}{2c\,(29.4)^2}\; 2\pi \times 0.4\, NH_0(1)(k\,\alpha\,R)\, {}_0\!\int^R J_0(k\,\alpha\,r)\, r^2\, \frac{(r/29.4)^{-0.75}(r/29.4+1)^{-3.25}}{(1+r/29.4 \times 11.4)}dr \qquad -(1)$$

b) Current field due to the annular ring of inner radius R and outer radius R_0 is given by.

$$E_c^{//}(R) = -\frac{ke10^5}{2c\,(29.4)^2}\,.\, 2\pi \times 0.4\, NJ_0(k\,\alpha\,R)\, {}_R\!\int^{Ro} H_0^{(1)}(k\,\alpha\,r)\, r^2\, \frac{(r/29.4)^{-0.75}(r/29.4+1)^{-3.25}}{(1+r/29.4 \times 11.4)}dr \qquad -(2)$$

Dipole field at a distance R from axis ($R < R_o$).

a) Dipole field due to the disc of radius R is given by

$$E_p^{/}(R) = ik\,\alpha\, e\tau\,\pi\, \frac{0.4N10^5}{R(29.4)^2} H_0(^1)(k\,\alpha\,R)\, {}_0\!\int^R J_0(k\,\alpha\,r)\, r^2\, \frac{(r/29.4)^{-0.75}(r/29.4+1)^{-3.25}}{(1+r/29.4 \times 11.4)}dr \qquad -(3)$$

b) Dipole field due to the annular ring of inner radius R and outer radius R_o is given by.

$$E_p^{//}(R) = ik\,\alpha\, e\tau\,\pi\, \frac{0.4N10^5}{R(29.4)^2} J_0^{/}(k\,\alpha\,R)\, {}_R\!\int^{Ro} H_0^{(1)}(k\,\alpha\,r)\, r^2\, \frac{(r/29.4)^{-0.75}(r/29.4+1)^{-3.25}}{(1+r/29.4 \times 11.4)}dr \qquad -(4)$$

The vector sum of $Ec^{/}$, $Ec^{//}$, $Ep^{/}$ & $Ep^{//}$ is the resultant field due to the geomagnetic mechanism.

In order to solve the problem of RE in the LF- MF- HF band, an encouraging suggestion was put forward by Nishimura in 1985(3).He proposed transition radiation (TR) mechanism as a possible source for LF-MF RE. A RE model for EAS on the basis of TR mechanism is developed by the GUCR group (4)

When shower particles hit the ground , the phenomenon of transition radiation must occur. The radiation field produced by the positive and negative charges of the moving dipole has a phase difference of (π + an additional term), the additional term is a function of Δ/λ where Δ is the lateral separation of the charges and λ is the wavelength of the radiation being considered. This additional phase change due to charge separation can be neglected for the LF-MF-HF region. Hence, all the charged particles may be assumed to be concentrated at a point instead of distribution over a disc for mathematical convenience, and only the excess negative charge, in effect, will contribute to the TR.

For a vertical air shower, the magnitude of the horizontal component of the field is

$$\vec{E}_{\omega H} = \frac{\varepsilon N e \lambda_1 \eta_1 \vec{k}}{2\pi^2 v \varsigma} \operatorname{Cos} \theta, \qquad - (5)$$

and the magnitude of the vertical component of the field is

$$\vec{E}_{\omega V} = \frac{\varepsilon N e \ \eta_1 k^2}{2\pi^2 v \varsigma} \operatorname{Cos}^2 \theta, \qquad -(6)$$

Where N = total number of shower particles at ground level,

$\varepsilon N e$ = excess negative charge,

$k = \omega/c = 2\pi v/c$ = wave number,

$$\lambda_1^2 = \frac{\omega^2}{c^2}\chi_1 - k^2 \ ; \ \chi_1 = \in_1 \mu_{1,}$$

$$\lambda_2^2 = \frac{\omega^2}{c^2}\chi_2 - k^2 \ ; \ \chi_2 = \in_2 \mu_{2,}$$

$$\eta_1 = \frac{\in_2/\in_1 - (v/\omega)\,\lambda_2}{k^2 - (\omega^2/c^2)\,\chi_1} + \frac{-1 + (v/\omega)\,\lambda_2}{k^2 - ((\omega^2/c^2)\,\chi_2}$$

$$\varsigma = \lambda_2 \in_1 + \lambda_1 \in_{2,}$$

$\tan\theta = Z / R$,

Z = height of the antenna from the ground.

R = distance of the antenna from the shower axis.

Different characteristics of RE studied:

(i) Frequency spectrum: Fig 3& 4

(ii) Variation of fieldstrength with age parameter & lateral distribution of fieldstrength : Fig. 5,6 & 7

(iii) TR model for inclined shower:

From the available experimental data of GU CR Research Laboratory at 120 KHz for inclined showers, the following important characteristics of inclined showers are studied.

(a) Variation of fieldstrength with zenith angle (φ) &

(b) lateral distribution of fieldstrength.

These are shown in figures 8,9, & 10 for $<E_p> = 5.6 \times 10^{15}$ eV, 4.9×10^{16} eV and 3.7×10^{17} eV respectively.

The transition radiation equation for vertical showers (eq^n 6) is modified on the basis of experimental observations presented in figures 8a (i) & (ii), 9a (i) & (ii) and 10a. The modified equations are –

For $<E_p> = 5.6 \times 10^{15}$ eV - (7)

$$\vec{E}_{\omega v} = (\varepsilon Ne\eta_1 k^2/4\pi^2\ v\varsigma)\ \mathrm{Cos}^2\ \theta - 0.09\ \phi,\ 70m \le R < 100m$$

$$\vec{E}_{\omega v} = (\varepsilon Ne\eta_1 k^2/4\pi^2\ v\varsigma)\ \mathrm{Cos}^2\ \theta - 0.11\ \phi,\ 30m < R < 70m$$

For $<E_p> = 4.9 \times 10^{16}$ eV - (8)

$$\vec{E}_{\omega v} = (\varepsilon Ne\eta_1 k^2/5.6\pi^2\ v\varsigma)\ \mathrm{Cos}^2\ \theta - 0.11\ \phi,\ 70m \le R < 100m$$

$$\vec{E}_{\omega v} = (\varepsilon Ne\eta_1 k^2/4.6\pi^2\ v\varsigma)\ \mathrm{Cos}^2\ \theta - 0.11\ \phi,\ 30m < R < 70m$$

For $<E_p> = 3.7 \times 10^{17}$ eV -(9)

$$\vec{E}_{\omega v} = (\varepsilon Ne\eta_1 k^2/5.2\pi^2\ v\varsigma)\ \mathrm{Cos}^2\ \theta - 0.11\ \phi,\ 70m < R < 100m$$

$$\vec{E}_{\omega v} = (\varepsilon Ne\eta_1 k^2/4\pi^2\ v\varsigma)\ \mathrm{Cos}^2\ \theta - 0.10\ \phi,\ 30m < R \le 70m$$

Where φ = zenith angle

R = Core distance

(iv) Comparision of Kahn & Lerche's model with Allan's model

(iv) Variation of Fieldstrength with Height of Shower Maximum (H_m)

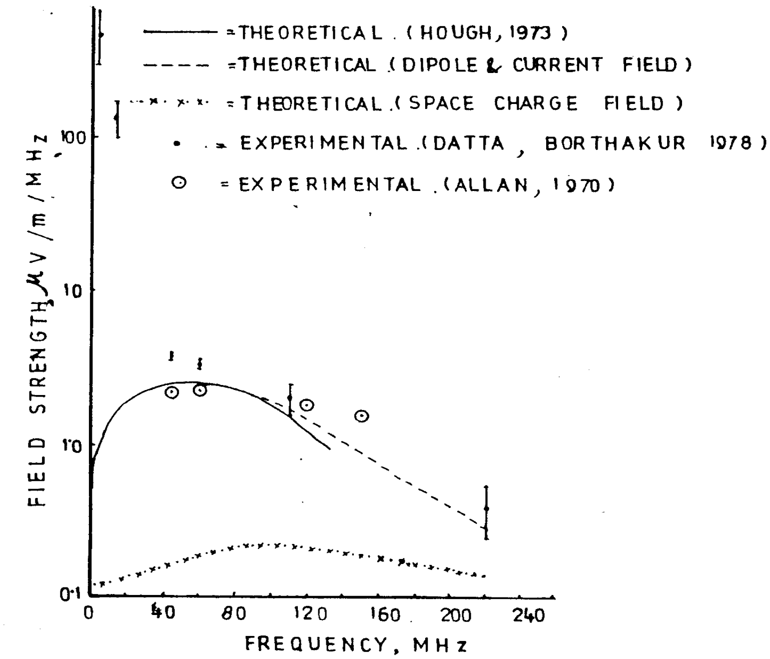

Fig. 3 - Variation of fieldstrength with frequency (Datta & Pathak, 1987)

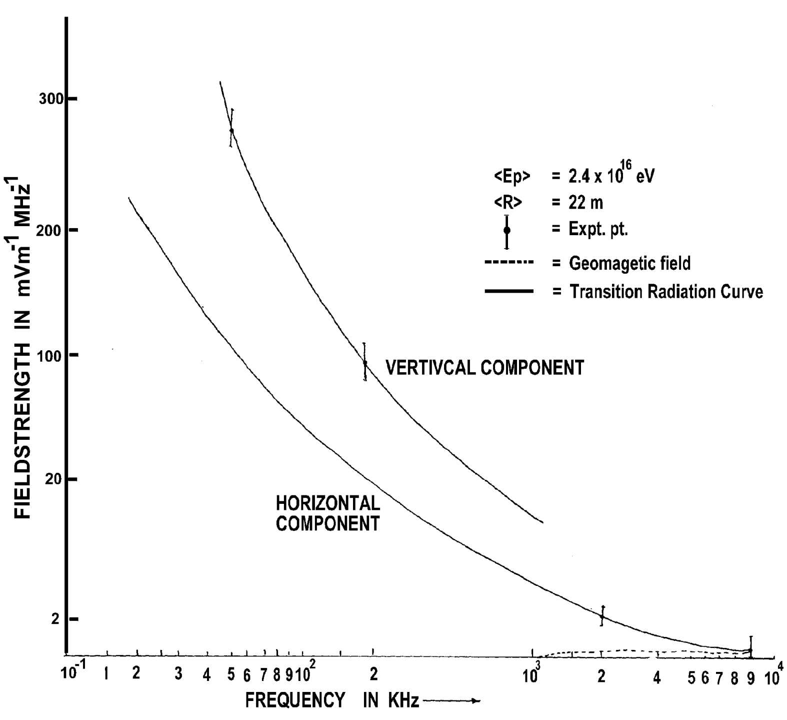

Fig. 4 Frequency spectra of LF-MF-HF radioemission.

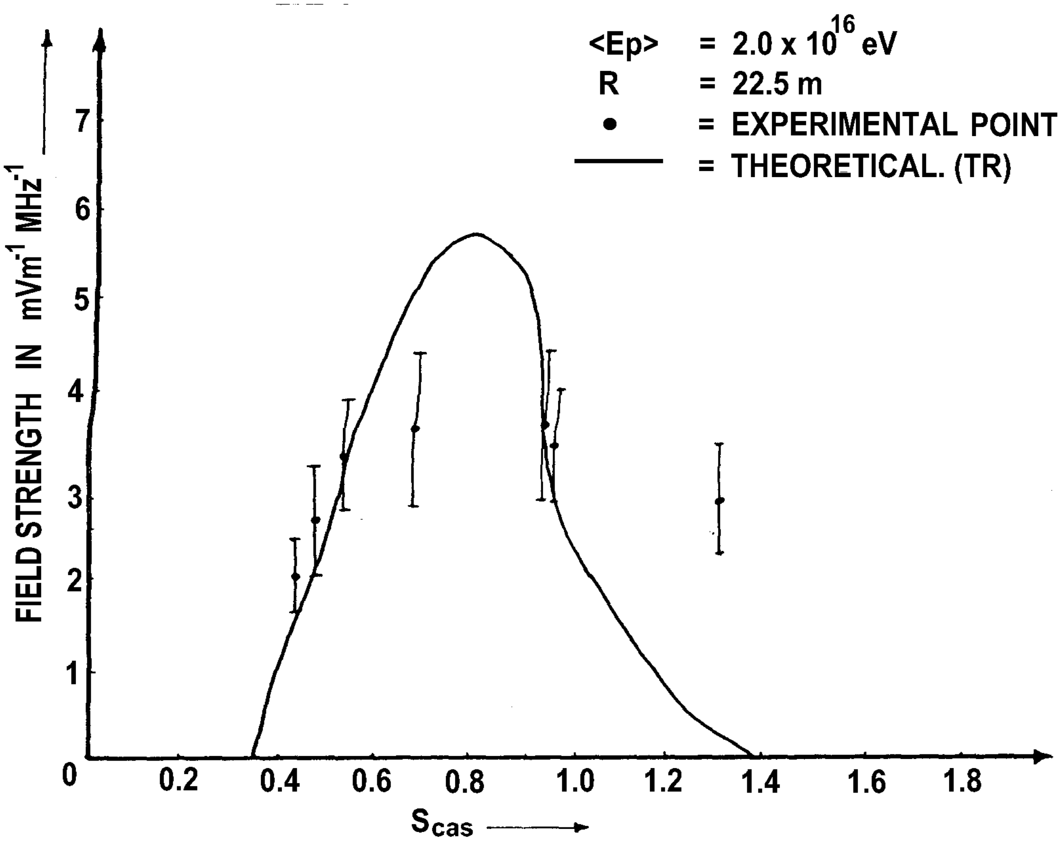

Fig. 5a - Field strength - S_{cas} curve at 2MHz Frequency.

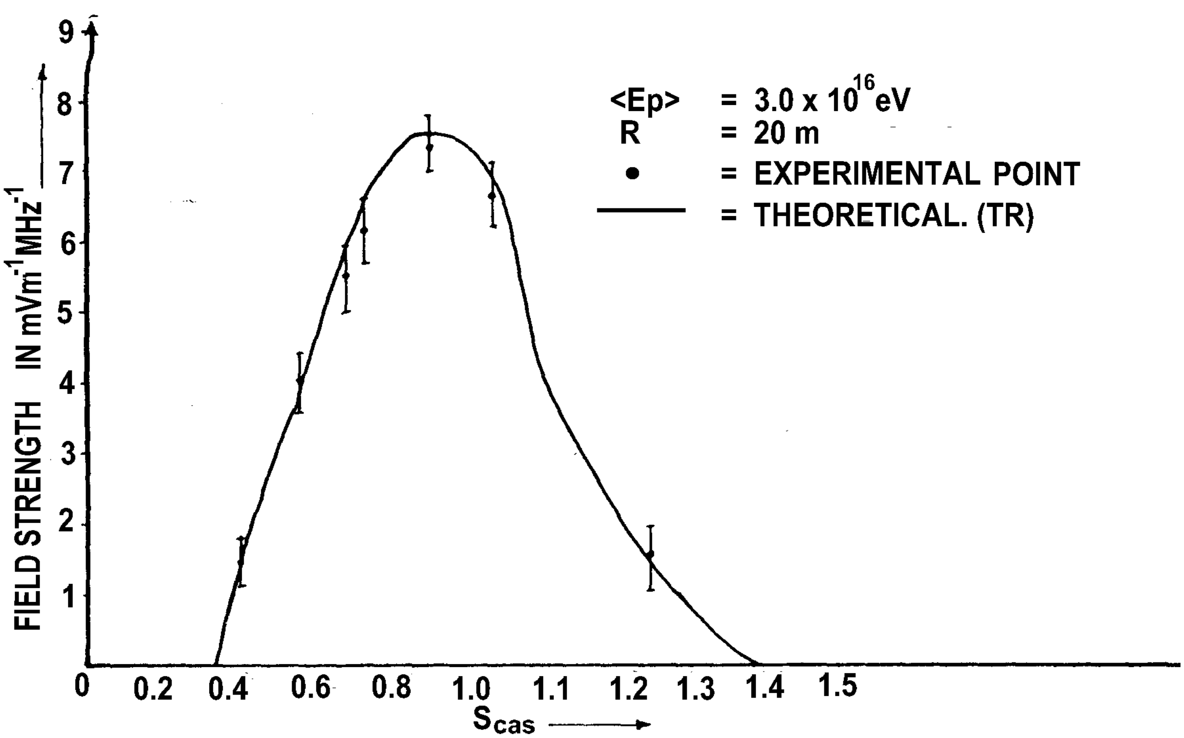

Fig. 5b - Field strength - S_{cas} curve at 2 MHz Frequency

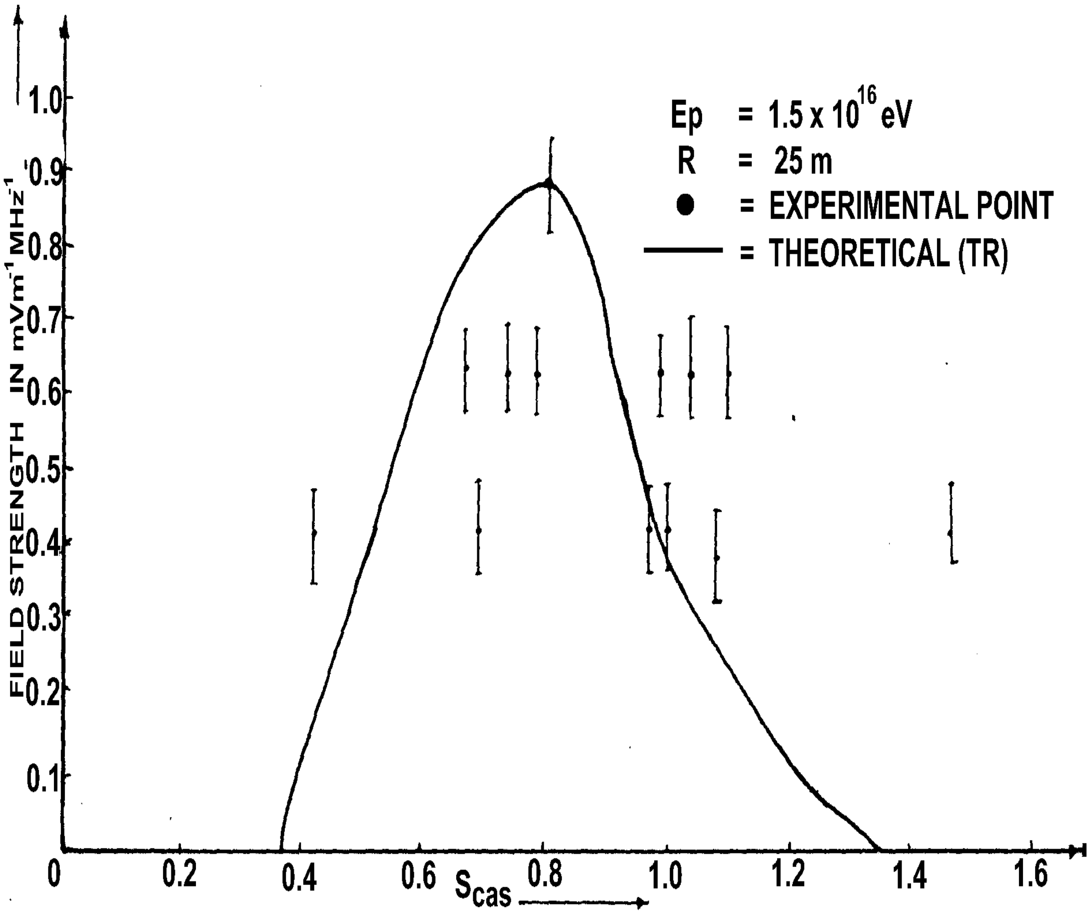

Fig. 6a - Field strength - S_{cas} curve at 9 MHz frequency

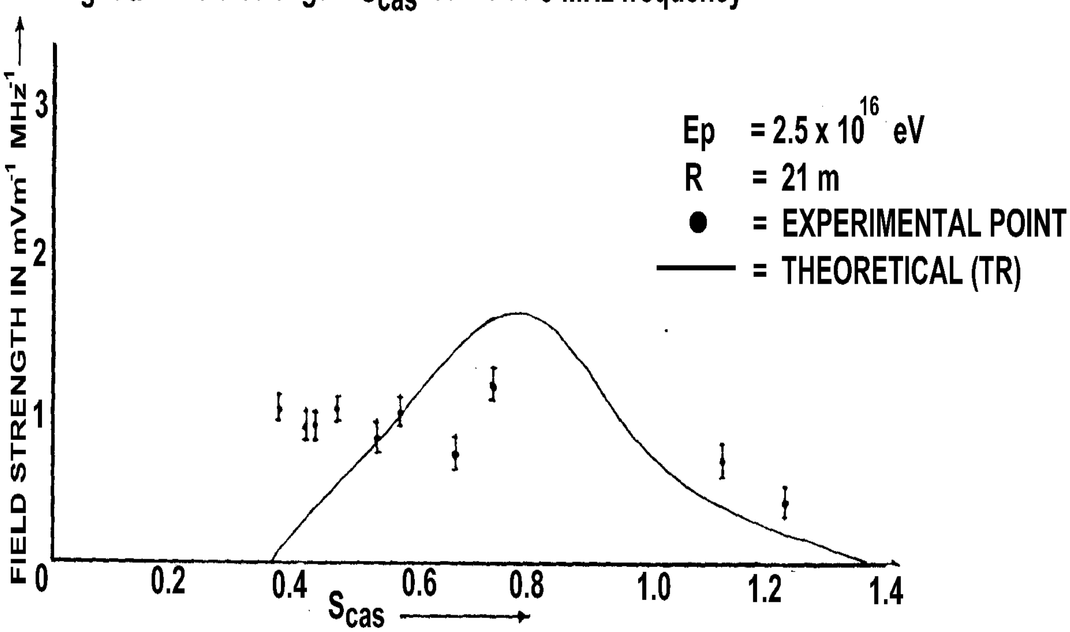

Fig. 6b - Field strength - S_{cas} curve at 9 MHz frequency

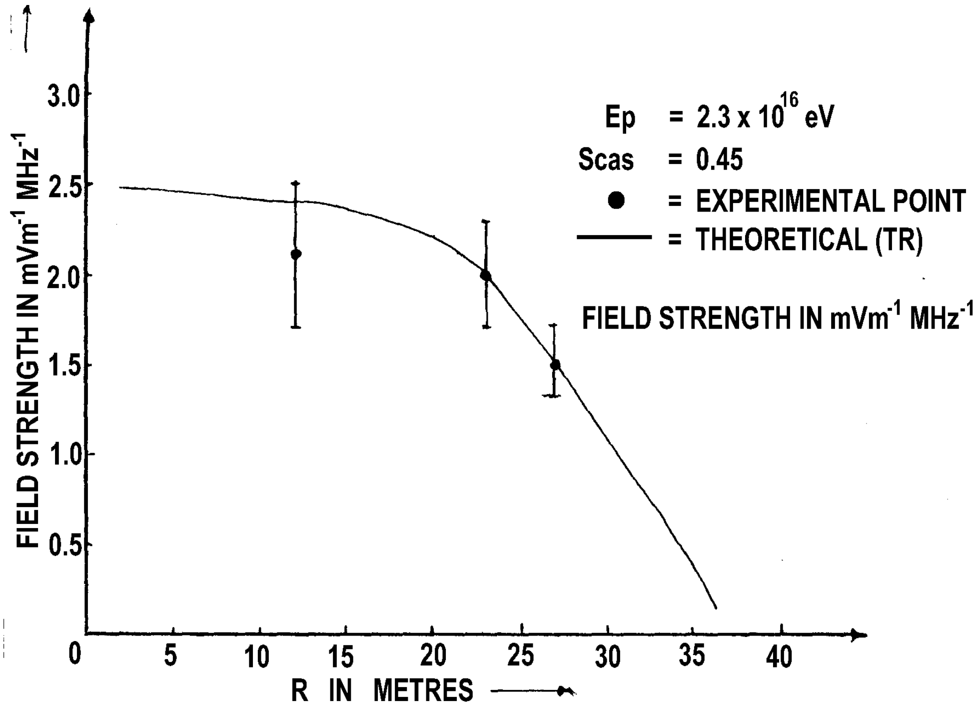

Fig. 7a - Lateral distribution of field strength at 2 MHz frequency

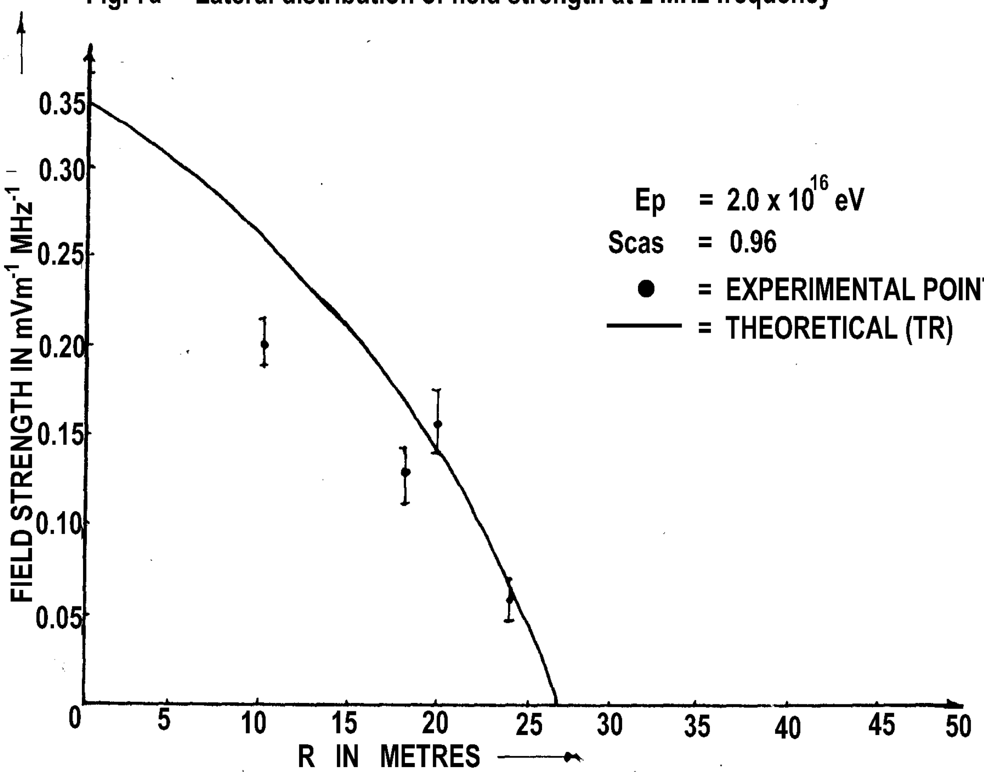

Fig. 7b - Lateral distribution of field strength at 2 MHz frequency

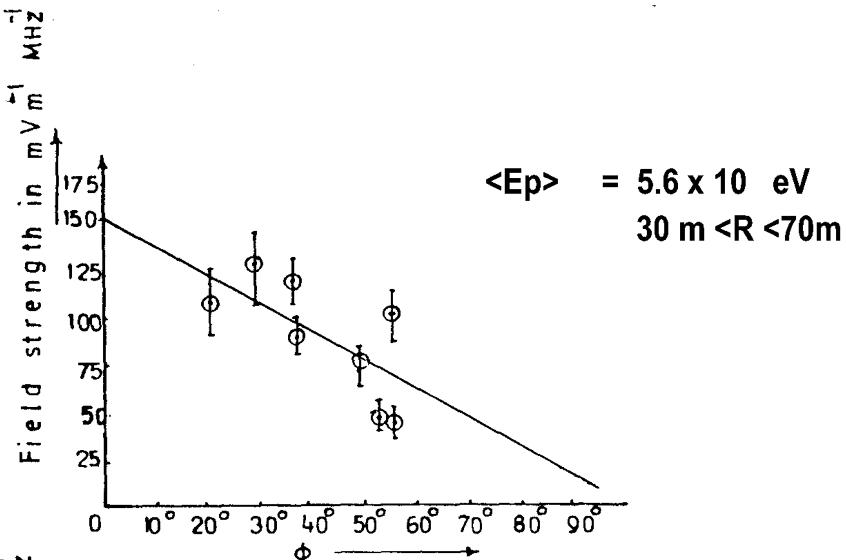

Fig. 8 a(i)-Variation of Field Strength with ø

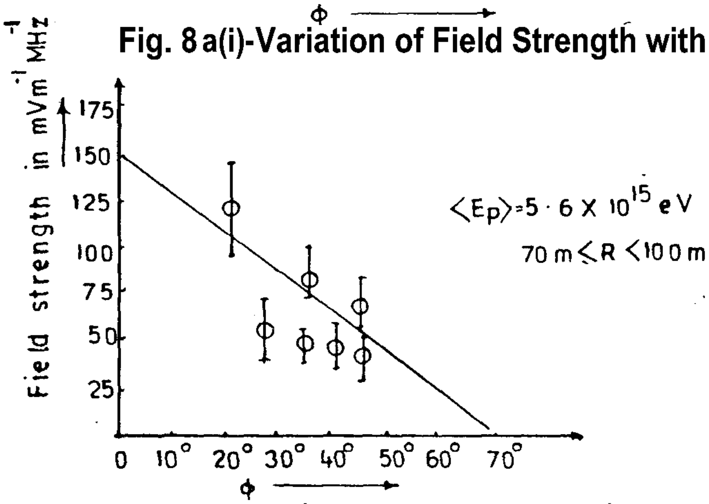

Fig.8 a(ii)-Variation of Field Strength with ø

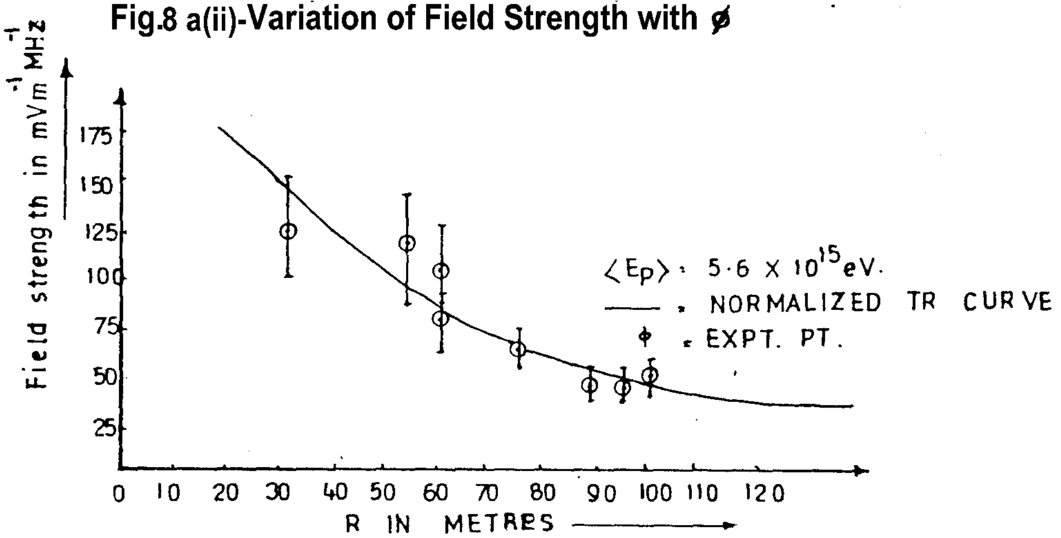

Fig. 8 b - Lateral Distribution of Field Strength

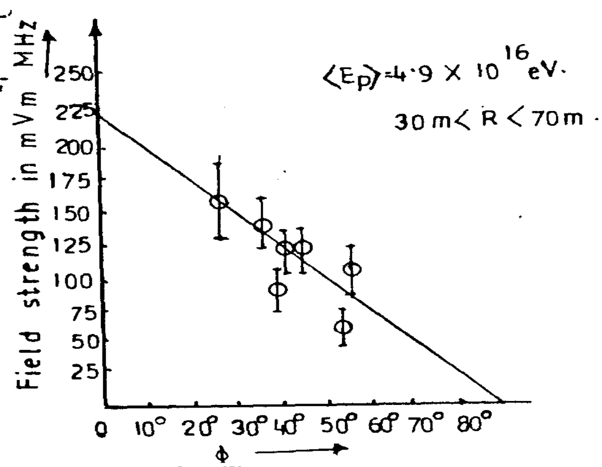

Fig. 9 a(i) - Variation o Field Strength with ø

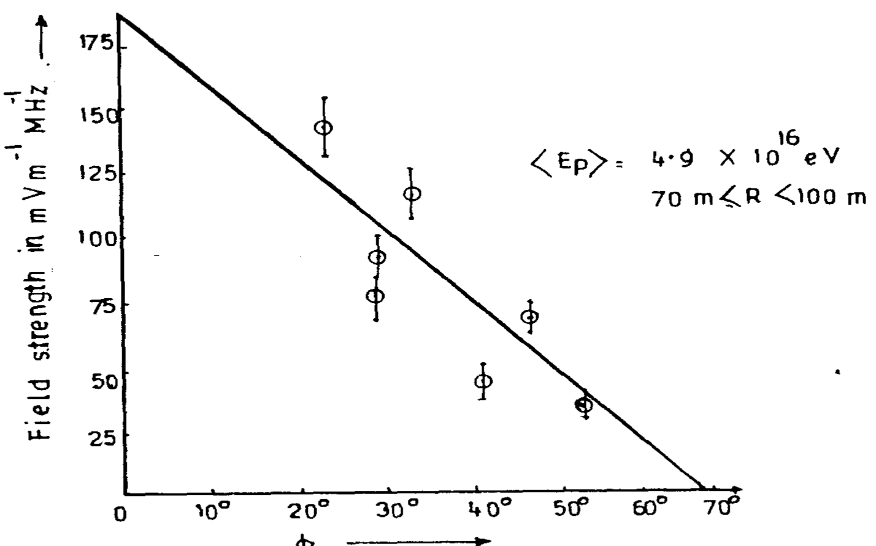

Fig. 9 a(ii) - Variation o Field Strength with ø

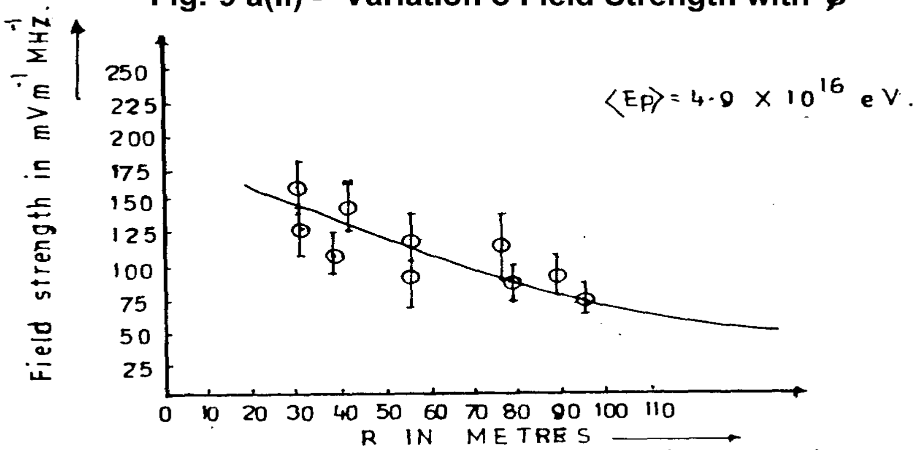

Fig. 9 b - Lateral distribution of Field strength

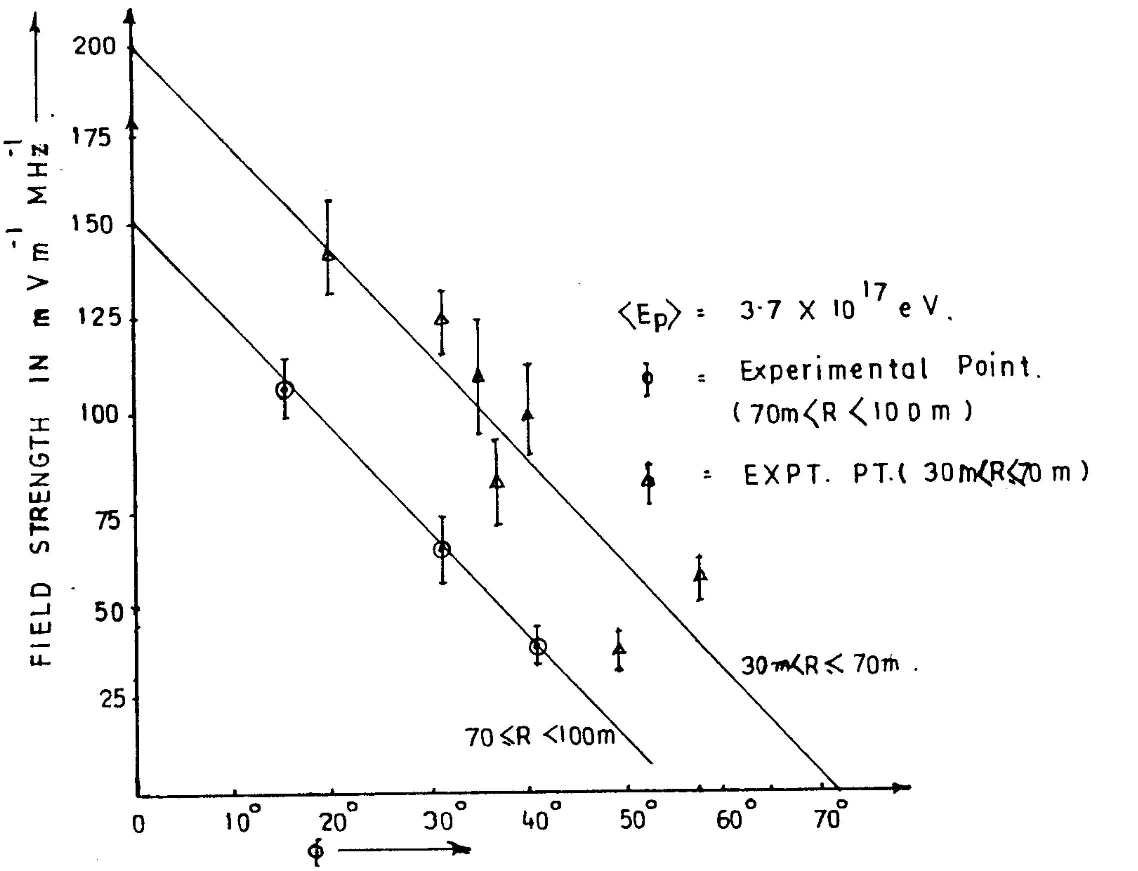

Fig. 10 a - Variation of Field Strength with Zenith Angle ø

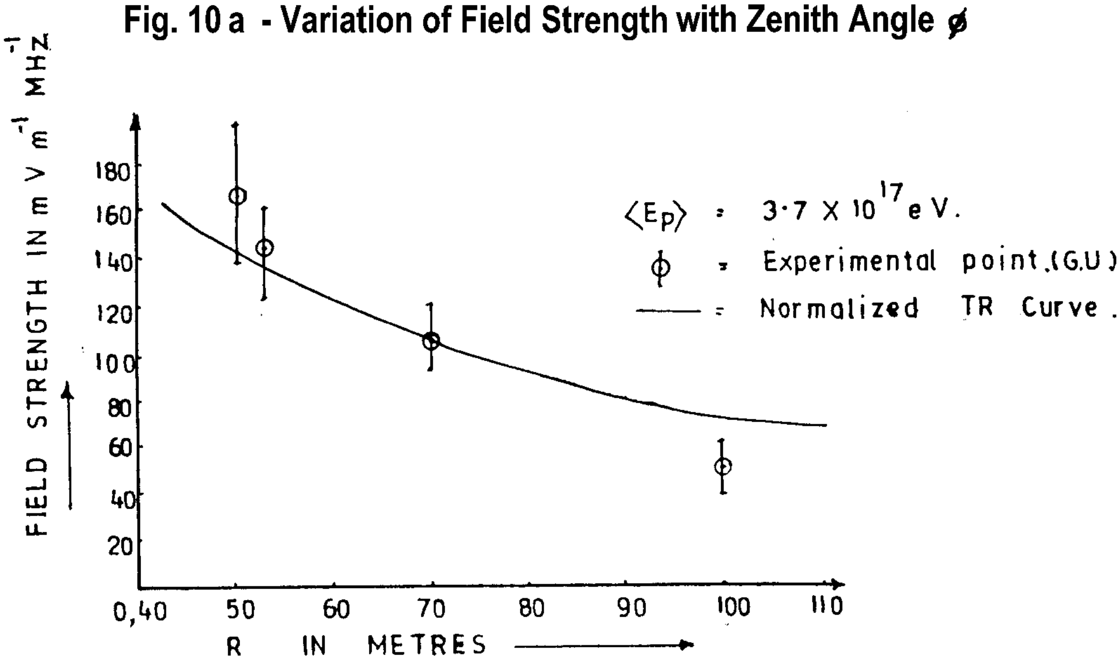

Fig. 10 b - Variation of Field Strength with core distance

Discussion on LF-MF-HF RE:

For a near vertical shower : The TR model exhibits a sharp increase of fieldstrengths with lowering of frequency whereas geomagnetic mechanism shows a slow decrease of fieldstrength with lowering of frequency (fig 4). The trend of the experimental frequency spectrum is in support of the TR model. Moreover, the data are found to be in good agreement, within experimental error, with the TR model.

The fildstrengths at 2 MHz given by the TR model increase with s_{cas} reach a maximum and then decrease. These theoretical curves fit well with the experimental fieldstrengths within experimental error (fig.5).

The experimental lateral distribution of fieldstrength at 2 MHz is also in good agreement with the TR model (Fig. 7a).

At 9 MHz, experimental fieldstrengths are almost independent of s_{cas} and hence these are not in agreement with the (Fig. 6) TR model.

At 9 MHz, theoritical lateral distribution of fieldstrength does not agree with the experimental observations (Fig. 7b).

For Inclined Showers : Figs. (8b, 9b and 10b) show that TR model (eqns. 7, 8 and 9) for inclined showers developed on the basis of experimental observations presented in figures 8a (i, ii), 9a (i,ii) and 10a, satisfactorily explains the observed lateral distribution of fieldstrength at 120 KHz.

Hence, in the LF-MF band experimental observations can be explained by TR model. But in the HF band observed fieldstrengths can not be explained by the TR model only, it appears to have contribution from other sources as well.

Investigations made by other workers [5,6,7,8] are summarised in Table 3.

TABLE: 3. Investigations made by GUCR group in the VLF-LF-MF-HF band.

Group	Frequency	Primary Energy	Results	Conclusions regarding the production mechanism	Inferences
Suga & Nishi (1987) [5]	26 KHz to 300 Khz	- 10^{16}eVto - 10^{19}eV	Detected pulses are unipolar and negative	Longitudinal current hypothesis proposed by Suga [2] and Synchrotron radiation proposed by Sakata [3] are ruled out. TR is the most probable mechanism.	
Kakimoto et al. (1990) [6]	LF-MF	$N > 10^7$	Detected pulses are negative unipolar. Field intensity is higher by about two orders than that expected from TR mechanism.	Polarity of the detected pulses are in support of TR mechanism but field intensity is not in support of TR.	
Castagnoli et al. (1991) [7]	350-500 KHz & 1.8-5 KHz	5.5×10^{15}eV -5.0×10^{17}eV	Electric field intensity increases towards lower frequencies.	The use of a multi-antenna detector will allow to test emission mechanisms (for example transition radiation)	
Kadota et al. (1993) [8]	LF-MF	$10^{17.5}$ eV to $10^{18.5}$ eV	Mainly negative unipolar with positive unipolar & bipolar signals are detected.	Deceleration of excess negative charge due to ionisation loss and the effect of geolectric of field, but observed pulse widths can be explained.	

Table 3 shows that although these observations do not lead to any definite conclusion regarding the production mechanism of LF-MF-HF radioemission, yet most of the groups point out towards transition radiation as the most probable mechanism.

It is worth mentioning that in the present work different important characteristics of LF-MF-HF radioemission viz. Frequency spectrum, dependence of fieldstrength on age parameter and lateral distribution of fieldstrength are studied at four different frequencies with the same experimental setup, but in none of the experiments listed in Table 3 this type of multicharacteristic studies are made.

Discussion on VHF RE :

The theoretical frequency spectrum obtained by Hough (modified Allan's model) gives a smooth variation of fieldstrength with frequency – fieldstrength slowly increases, reaches a maximum and then decreases (fig 11). But the frequency spectrum obtained from the present theoretical work (modified Kahn & Lerche's model) seem to be quite unphysical, because it shows rapid fluctuation of fieldstrength with frequency which is not supported by experimental observations of any group.

At 110 MHz, the lateral distribution of fieldstrength given by modified Allan's model has quite opposite trend to that obtained from modified Kahn & Lerche's model. The exprimental data is in good agreement with modified Allan's model (fig 12)

The theoretical lateral distribution at 220 MHz, based on modified Kahn & Lerche's model is unphysical because it shows rapid fluctuation of fieldstrength with core distance. Experimental lateral distrubution shows a smooth variation of fieldstrength with core distance (fig 13)

The experimental observations on variation of fieldstrength with height of shower maximum (H_m) at 110 MHz agree, within experimental error, with theoretical calculations of modified Allan's model. On the other hand, calculations done on the basis of modified Kahn & Lerche's model is in total disagreement (fig 14)

The experimental observation on variation of fieldstrength with height of shower maximum (H_m) at 220 MHz also do not agree with modified Kahn & Lerche's model .

Hence, it is obvious that the two models of radioemission from EAS cannot be regarded as equivalent to each other. Allan's model. Which is microscopic in concept, is more realistic.

Fig 15 and `t`- test for correlation co-efficient at 110 and 220 MHz indicate that for showers having s_{cas} <1, no correlation exist between fieldstrength and s_{cas} at both the frequencies in the VHF band. (Fieldstrength -H_m) curves at 110 MHz & 220 MHz indicate that for old showers (s_{cas} >1) there exist a correlation between fieldstrength and $H_{m.}$ Thus, for old showers the resultant effect of both the growth and decay must be taken into account in calculating the fieldstrength of radioemission.

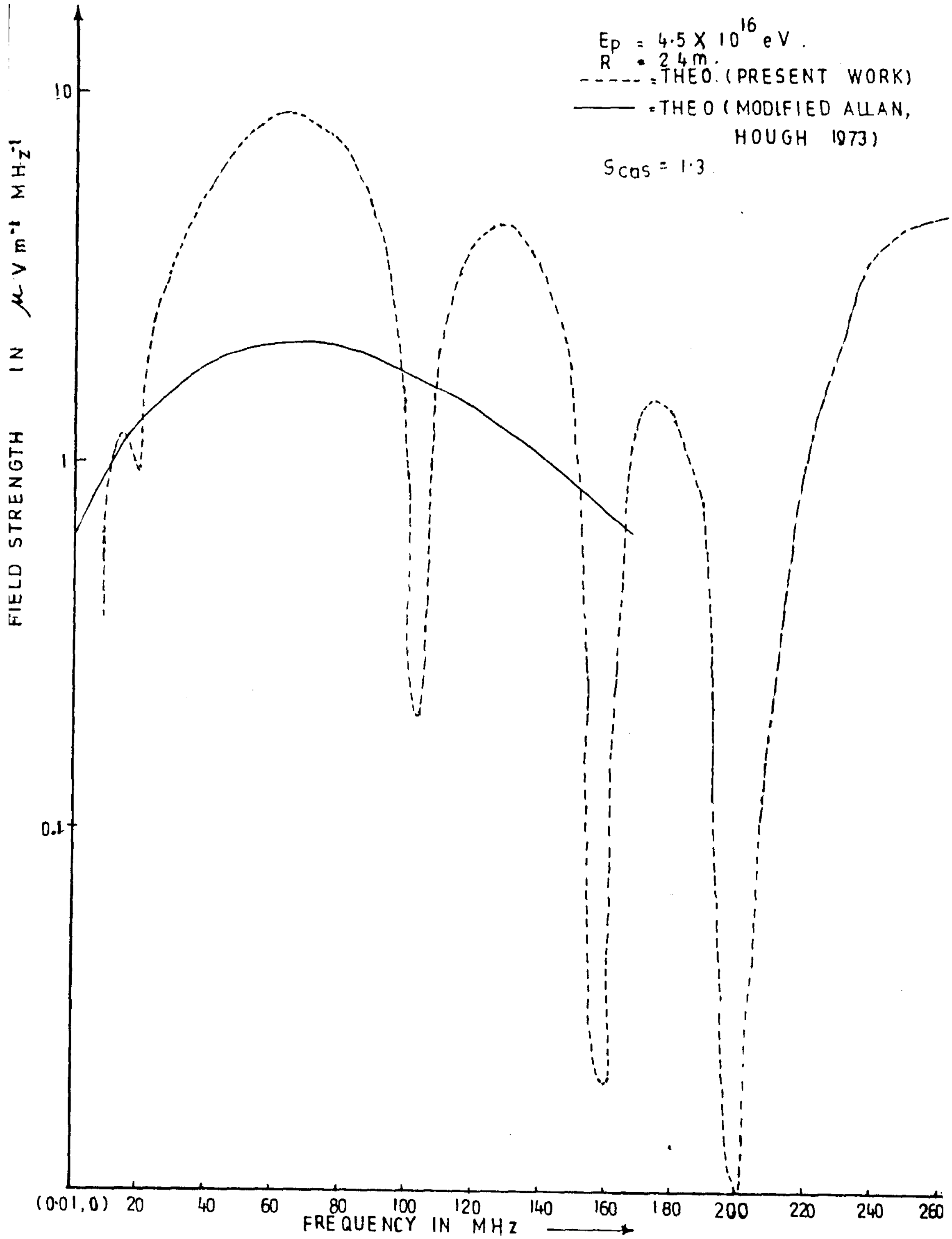

Fig. 11 - Frequency spectra of radioemission

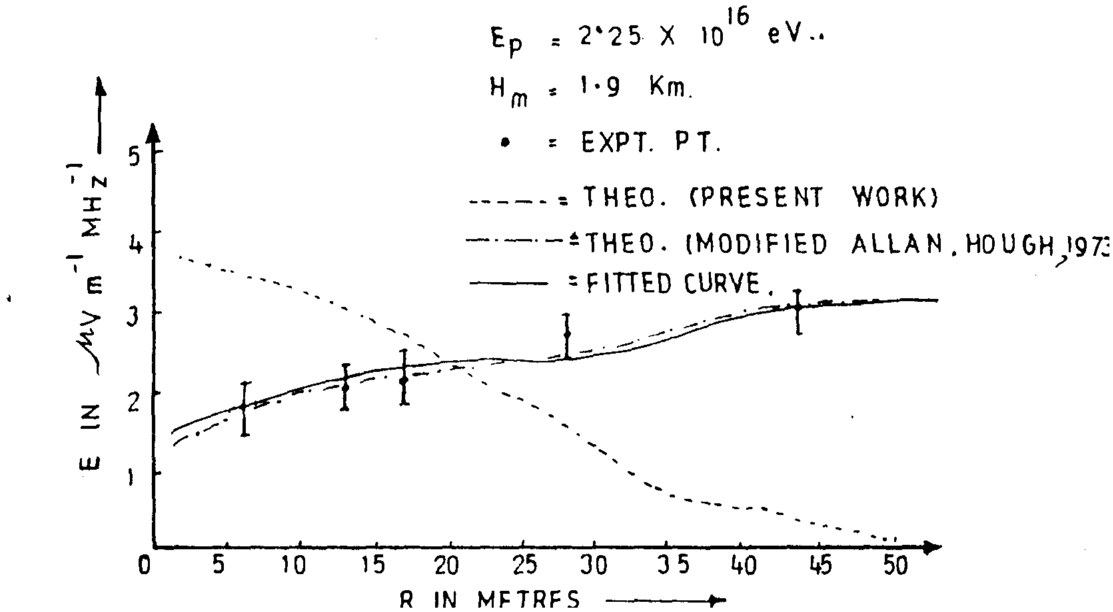

Fig. 12 - Lateral distribution of fieldstrength (E) at 110 MHz Frequency

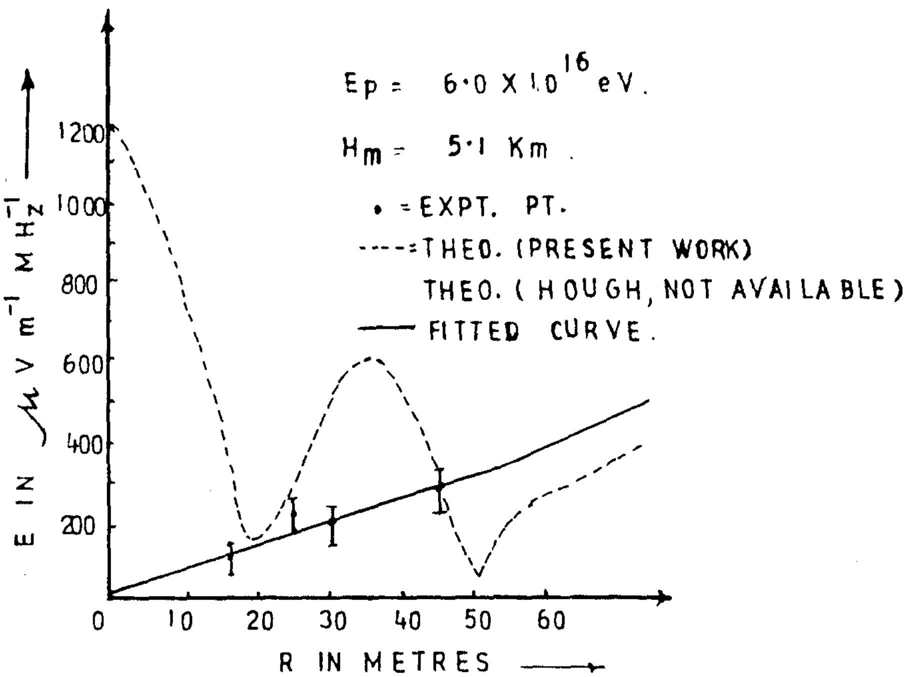

Fig. 13 - Lateral distribution at field strength (E) at 220 MHz frequency

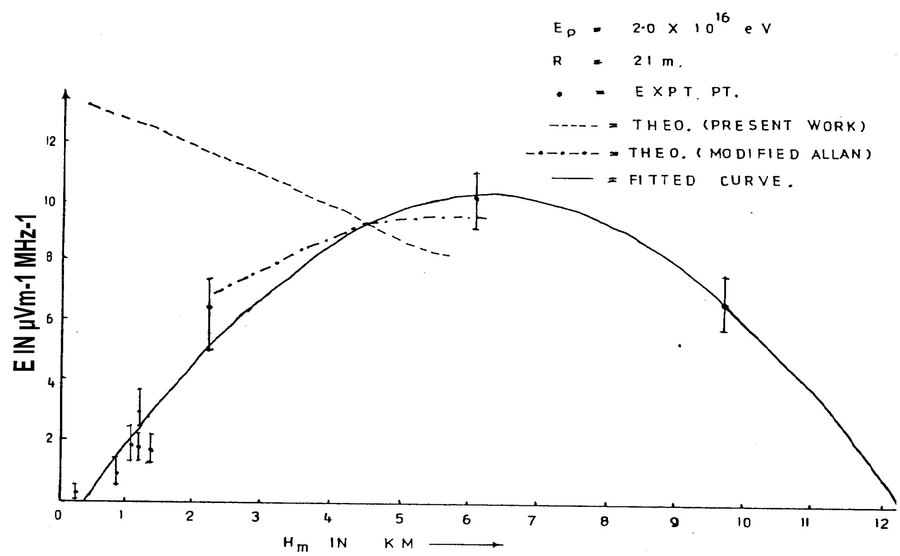

Fig. 14 - Field strength (E) - Height of shower maximum (H_m) curve at 110 MHz frequency

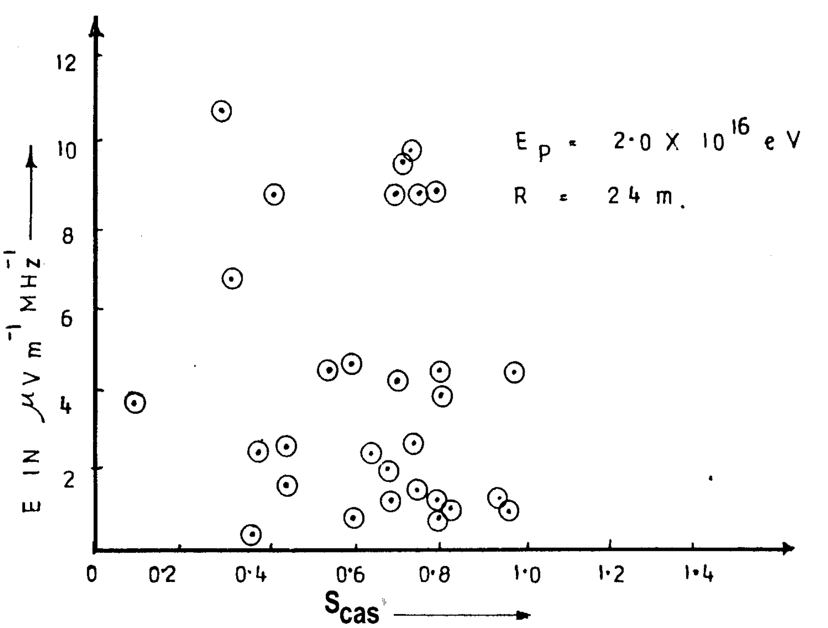

Fig. 15 - Field strength (E) - Age Parameter S_{cas} (S_{cas}<1) at 110 MHz frequency

Conclusion: This investigation can be summarized in the form of the following conclusions :

(i) In the LF-MF band experimental observations for near vertical showers can be explained by the TR model developed by the group.
(ii) In the HF band , TR is not solely responsible for radioemission.
(iii) TR model developed for inclined showers on the basis of experimental observations at 120 KHz is found to be adequate.
(iv) Modified Kahn & Lerche's model and modified Allan's model are not equivalent to each other. Modified Allan's model is more realistic than Kahn & Lerche's model.
(v) In the VHF band, no correlation exists between fieldstrength and s_{cas} for $s_{cas}<1$.
(vi) Showers with age parameter $s_{cas}>1$ can be employed to estimate primary mass composition by radio method in the VHF band.
(vii) Since observed characteristics of LF-MF Radioemission from EAS indicates very high fieldstrengths,for neutrino detection better results may be expected if frequency of observationis shifted to LF-MF from VHF band. Moreover, in major projects like Pierre-Auger observatory, VLF-LF radio detection may be considered as another technique for Giant Shower studies, which was suggested by Prof. Suga about two decades ago.

Acknowledgement:

This piece of work is the outcome of the contributions towards CR research of all the members, present and past, of the GUCR group. They are, therefore, thankfully acknowledged.

REFERENCES:

1. Castagnoli C et al., Nuovo Cimento (Italy), 63 (1969), 373.
2. Kahn F.D. & Lerche I., Proc. R Soc. London Ser A (GB), 289(1966),206.
3. Nishimura J., Proc.19th ICRC,La Jolla, USA,Vol. 7, (1985),308.
4. Baishya R. et al., II Nuovo Cimento. Vol 16 C,N. 1. (1992),17.
5. Suga K. & Nishi K, Proc. 20th ICRC, 6, Moscow.
6. Kakimoto F., Umezawa T.,Nishiyama T.,and Nishi K.(1990).Proc, 21st ICRC Adelaide,9,213.
7. Castagnoli C., Ghia p.l.,Gomez F. and TriveroP.(1991),Proc,22nd ICRC, Dublin,4,363.
8. Kadota K, Suzuki Y., Nishi K. and Kakimoto F, (1993), Proc. 23rdICRC, Calgary, 4 262.